

Classification of Links in $\mathbb{R}P^3$ with at Most Six Crossings

JULIA DROBOTUKHINA

§1. Introduction

A *link* in real projective space $\mathbb{R}P^3$ is a one-dimensional closed smooth submanifold $L \subset \mathbb{R}P^3$. By an (*ambient*) *isotopy* of L we mean a smooth homotopy $h_t: L \hookrightarrow \mathbb{R}P^3$ with $t \in [0, 1]$, where h_0 is the inclusion $L \rightarrow \mathbb{R}P^3$. Two links L_1, L_2 are (*ambiently*) *isotopic* if there exists an isotopy h_t ($t \in [0, 1]$) of L_1 such that $h_1(L_1) = L_2$. One of the first problems of link theory in $\mathbb{R}P^3$ is the problem of classification of links in $\mathbb{R}P^3$ up to isotopy.

Links in $\mathbb{R}P^3$, as well as links in \mathbb{R}^3 , can be presented by special plane pictures, which are called *diagrams*. Diagrams of links in $\mathbb{R}P^3$ differ from diagrams of links in \mathbb{R}^3 in that a diagram of a link in $\mathbb{R}P^3$ is placed not in the plane, but in a disk; arcs of the diagram meet the boundary of the disk in pairs of antipodal points. The moves $\Omega_1 - \Omega_5$ of diagrams (see Figure 1 on the next page) correspond to link isotopy. The moves $\Omega_1 - \Omega_3$ coincide with the classical Reidemeister moves. For details see [D1].

In this article links in $\mathbb{R}P^3$ that can be presented by diagrams with at most six crossings are classified up to isotopy and homeomorphism. Here, as in the classification of links in \mathbb{R}^3 , we exclude from consideration *reducible links*, i.e., links which are (nontrivial) connected or disjoint sums. We exclude also *affine links*, i.e., links that can be placed in an affine part on $\mathbb{R}P^3$ by an isotopy, since their classification coincides with classification of links in \mathbb{R}^3 .

For the classification of links in $\mathbb{R}P^3$ one needs to enumerate diagrams that represent all isotopic types of links in $\mathbb{R}P^3$ with a given number of double points, and to prove that links in the list obtained are pairwise nonisotopic. The latter demands calculation of some link invariants. To obtain a complete list of diagrams of links in $\mathbb{R}P^3$, we use an approach that was proposed by Conway [C] for the enumeration of diagrams of links in \mathbb{R}^3 ; see §2. The main invariant for nonoriented links in $\mathbb{R}P^3$ is a polynomial generalizing the

1991 *Mathematics Subject Classification*. Primary 57M25.

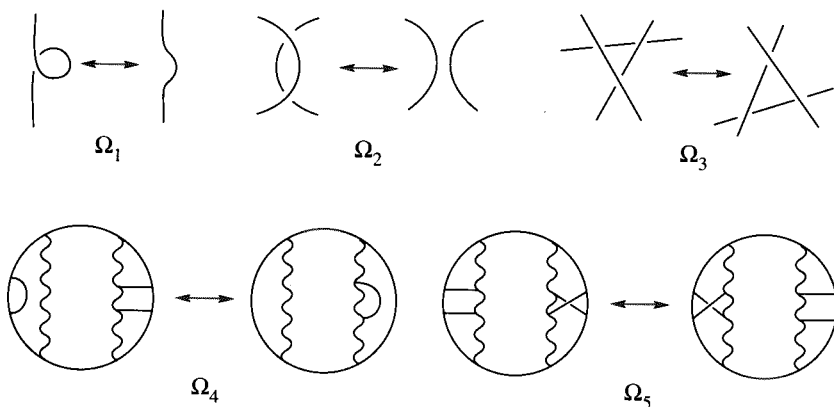


FIGURE 1

Jones polynomial (in Kauffman's version) of classical links. This polynomial slightly differs from the polynomial introduced in [D1]; for the definitions of these polynomials see subsection 3.1. Apart from this, we use the results of [D2], where projective Montesinos links are classified.

§2. Enumeration of diagrams

2.1. Tangles. By a *tangle* we mean a part of a link diagram placed in a disk and intersecting (transversally) the boundary of the disk in four points lying on orthogonal diameters. An example of a tangle is shown in Figure 2. Two tangles are said to be *equivalent* if they can be transformed to one another by a sequence of Reidemeister moves with the end points of tangles fixed.

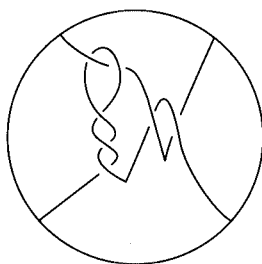


FIGURE 2

By the *sum* $t_1 + t_2$ of tangles t_1 and t_2 , we mean the tangle constructed from t_1 and t_2 in the way shown in Figure 3.

By the *product* $(t_1 t_2)$ of tangles t_1 and t_2 we mean the tangle $t'_1 + t_2$, where t'_1 is the tangle obtained from t_1 by reflection in the line passing through the boundary points p_1 and p_3 (see Figure 4).

By *integer tangles* n , $-n$ ($n \in \mathbb{N}$), and 0 , we mean the tangles shown in Figures 5a, 5b, and 5c respectively. The tangle shown in Figure 5d is denoted by the symbol ∞ .

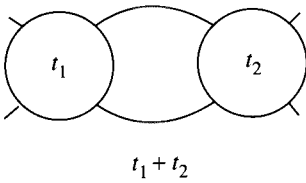


FIGURE 3

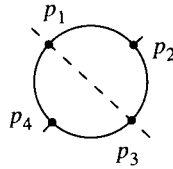
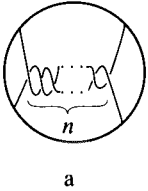
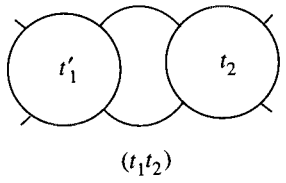
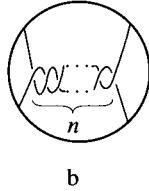


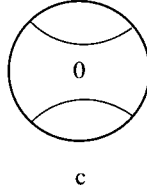
FIGURE 4



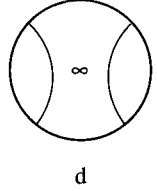
a



b



c



d

FIGURE 5

A tangle obtained from the tangles $0, \infty, 1, -1$ by summation and multiplication is said to be *algebraic*.

The product $(\dots(i_1 i_2) i_3 \dots i_n)$ of integer tangles i_1, \dots, i_n is called a *rational tangle* $i_1 \dots i_n$.

Conway [C] showed that two rational tangles $i_1 \dots i_n$ and $j_1 \dots j_m$ are equivalent if and only if the corresponding continued fractions

$$i_n + \frac{1}{i_{n-1} + \frac{1}{i_{n-2} + \dots + \frac{1}{i_1}}}, \quad j_m + \frac{1}{j_{m-1} + \frac{1}{j_{m-2} + \dots + \frac{1}{j_1}}}$$

have the same value (it is understood that $1/0 = \infty, 1/\infty = 0, k + \infty = \infty$ for $k \in \mathbb{Z}$). It follows that any rational tangle different from $0, \infty, 1, -1$ can be reduced to the following standard form: either $i_1 \dots i_n$ or $i_1 \dots i_n 0$, where $|i_1| \geq 2$ and all the i_1, \dots, i_n are nonzero integers of the same sign. The rational tangle $i_1 \dots i_n$ with

$$i_n + \frac{1}{i_{n-1} + \frac{1}{i_{n-2} + \dots + \frac{1}{i_1}}} = p/q \in \mathbb{Q}$$

is called a p/q tangle.

2.2. Nets. A *net* is by definition the image in $\mathbb{R}P^2$ of several circles under an immersion in general position. In particular, a connected net is either a circle embedded in $\mathbb{R}P^2$ or a connected graph embedded in $\mathbb{R}P^2$, all vertices

of which are 4-valent. To any diagram of a link in $\mathbb{R}P^3$ corresponds a net in the projective plane obtained from the disk of the diagram by identification of antipodal points of the boundary circle.

A net is said to be *contractible* if its inclusion in $\mathbb{R}P^2$ is homotopic to a constant map.

A net s is said to be *irreducible* if for any circle embedded in $\mathbb{R}P^2$, intersecting s (transversally) at exactly two points, and dividing $\mathbb{R}P^2$ into a disk D and a Möbius strip M , either $s \cap D$ is a simple arc, or $s \cap M$ is a simple arc dividing M .

A net is said to be *base* if it is connected, noncontractible, irreducible, and none of the regions into which it divides $\mathbb{R}P^2$ has exactly two vertices on its boundary.

A diagram of a link in $\mathbb{R}P^3$ is said to be *base* if the corresponding net is base.

By a *base graph* we mean a base diagram with overpasses and underpasses ignored. Two base graphs determine the same base net if they are obtained from one another by a series of moves $\tilde{\Omega}_4$, $\tilde{\Omega}_5$ corresponding to Ω_4 , Ω_5 (see Figure 6).

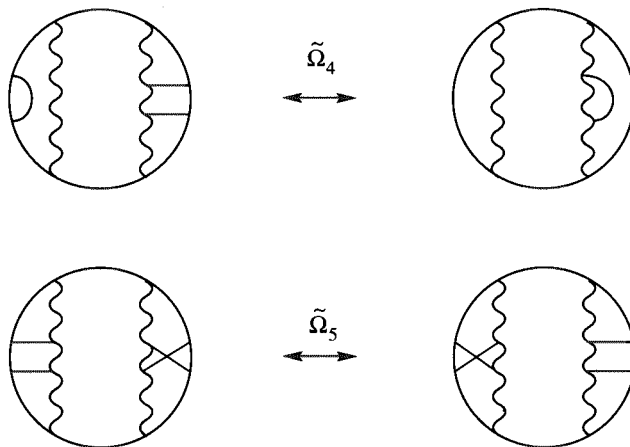


FIGURE 6

2.3. Enumeration of links. A diagram is said to be *reduced* if there is no circle whose embedding in $\mathbb{R}P^2$ is two sided and intersects the net of the diagram at two points exactly near a double point (see Figure 7).

Removing a small neighborhood of each vertex of the base graph and inserting an algebraic tangle in its place gives a diagram of a link in $\mathbb{R}P^3$.

LEMMA (cf. [C]). *Any reduced diagram of an irreducible nonaffine link in $\mathbb{R}P^3$ can be transformed by moves Ω_4 , Ω_5 to a diagram that can be obtained by inserting algebraic tangles distinct from 0 and ∞ in place of vertices of some base graph. The corresponding base graph (considered up to $\tilde{\Omega}_4$, $\tilde{\Omega}_5$),*

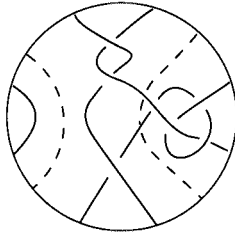


FIGURE 7

the algebraic tangles, and the insertion process are determined by the original diagram uniquely.

PROOF. Here is the process of constructing the base graph from a link diagram. Let Γ be the net of the diagram D . Since the link is irreducible and nonaffine, Γ is connected and nondividing. Since the link is irreducible and the diagram is reduced, Γ is irreducible. If Γ divides $\mathbb{R}P^2$ into regions none of which has exactly two vertices in its boundary, then Γ is a base net. Assume now that among these regions there is one whose boundary contains exactly two vertices (we call it a *lune*). Applying, if necessary, the moves Ω_4 and Ω_5 , one can make the lune disjoint with the projective line corresponding to the boundary of the disk of the diagram. Contract the lune to a point. We obtain a new net Γ_1 . Its vertices are in the complement of the projective line. It is clear that Γ_1 is connected and noncontractible. Γ_1 is irreducible since Γ is irreducible (see Figure 8). If among the regions into which Γ_1 divides $\mathbb{R}P^2$ there are no lunes, then Γ_1 is a base net. Otherwise we contract one of the lunes, having applied, if necessary, Ω_4 , Ω_5 to the diagram with net Γ_1 to put the lune in the complement of the projective line. We obtain a new net Γ_2 . The contracting process is applied until all lunes disappear. It is clear that the net obtained does not depend on the sequence of contractions and is a base net.

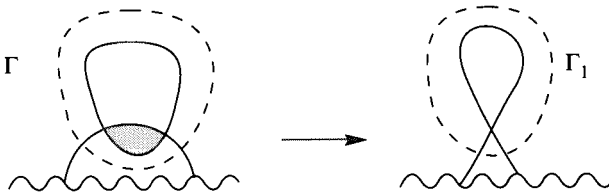


FIGURE 8

The base net determines a base graph up to $\tilde{\Omega}_4$, $\tilde{\Omega}_5$. We insert the corresponding algebraic tangles in place of its vertices obtained from contracted regions and the tangles 1 or -1 on the other vertices to restore D . We obtain a diagram that differs from D by a sequence of moves Ω_4 , Ω_5 . An

example of the contracting process is shown in Figure 9 (near vertices, the algebraic tangles to be inserted are shown).

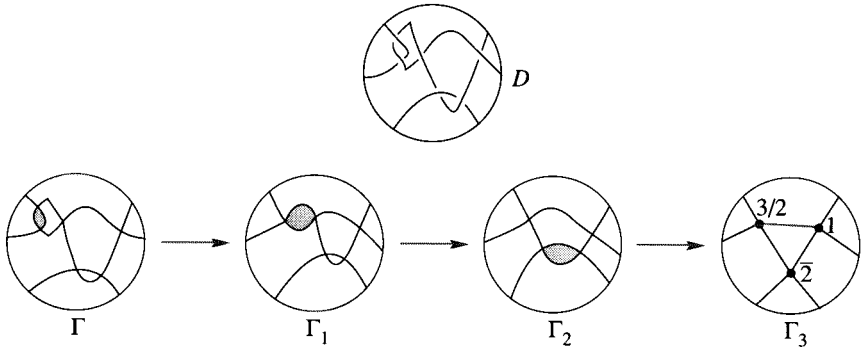


FIGURE 9

The construction shows that the base graph (up to $\tilde{\Omega}_4, \tilde{\Omega}_5$), the algebraic tangles, and the insertion process are determined in a unique way.

THEOREM. *To enumerate all irreducible nonaffine links in $\mathbb{R}P^3$ that can be presented by diagrams with at most n double points, it is sufficient to enumerate all base nets with at most n vertices, all algebraic tangles with at most n double points, and for each of the enumerated base nets take the corresponding base graph and enumerate all possible ways of inserting the tangles in place of vertices of the graph so that the result is a diagram with at most n double points.*

PROOF. This theorem follows immediately from the lemma, because the moves Ω_4, Ω_5 do not change the number of double points of a diagram.

2.4. Enumeration of base nets. A region in $\mathbb{R}P^2$ bounded by edges of a net is called an n -gon if exactly n vertices lie on the boundary of this region.

LEMMA 1. *Let $v \geq 3$ be the number of vertices of a base net Γ , e be the number of its edges, and d be the number of regions into which Γ divides $\mathbb{R}P^2$. Let d_3, d_4, \dots, d_v be the number of triangles, quadrangles, \dots , v -gons respectively among these d regions. Then*

$$\left. \begin{aligned} d &= v + 1, \\ d &= d_3 + d_4 + \dots + d_v, \\ 2e &= 3d_3 + 4d_4 + \dots + vd_v. \end{aligned} \right\} (*)$$

PROOF. First note that when $v \geq 3$, none of the regions into which the net divides $\mathbb{R}P^2$ has exactly one vertex on its boundary (this follows from the irreducibility of the net). Since $v - e + d = \chi(\mathbb{R}P^2) = 1$ and $4v = 2e$, we have $d = v + 1$. The second and third equalities of (*) are obvious.

LEMMA 2. *If n is even, there is no base net with n vertices containing the n -gon. If n is odd, there exists only one such net.*

PROOF. Let Γ be a net with n vertices containing the n -gon N . Consider an edge e of Γ not belonging to N . Denote by α the cycle in Γ formed by e and the edges of N . Let us show that if α is a two-sided embedded circle, then Γ is not a base net. Denote by D the disk bounded by α . Put

$$D_0 = \begin{cases} D & \text{if } N \not\subset D, \\ \text{Cl}(D \setminus N) & \text{if } N \subset D. \end{cases}$$

The disk D_0 contains the graph $\Gamma' = D_0 \cap \Gamma$, all vertices of which lie in ∂D_0 . If the number of vertices of N is greater than two, there is a vertex $v \in \Gamma'$ not lying in e . An edge e_1 with $\text{Int } e_1 \subset \text{Int } D_0$ and a vertex v divides D_0 into two parts. Denote by D_1 the closure of the part that does not contain e . The boundary of D_1 consists of several edges of N and e_1 , and contains less vertices than the boundary of D_0 . Applying to D_1 the same argument as to D_0 , we obtain a new region D_2 having less vertices, and so on. It is clear that at some step the next region D_k ($D_k \subset D_{k-1} \subset \dots \subset D_1 \subset D_0$) will have in its boundary either one or two vertices. This means that Γ is not a base net.

Thus Γ can be a base net only in the case if for any edge $e \notin N$ the cycle α formed by e and some edges of N is the image of a one-sided embedding of the circle. The net satisfying this condition is unique (see Figure 10). It is not a base net in the case of even n and is a base net in the case of odd n . \square

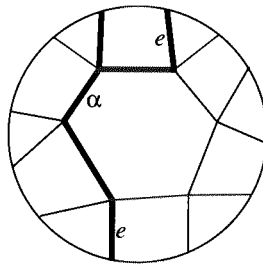


FIGURE 10

BASE NETS WITH NO MORE THAN FOUR VERTICES. *Obviously, there exists only one base net with one vertex; the corresponding base graph is shown in Figure 11a.*

Note that this net is the only one with a vertex to which only two components of the complement are adjacent. In any other base net, at each vertex there are four different adjacent components of the complement and each component of the complement is a polygon embedded in $\mathbb{R}P^2$.

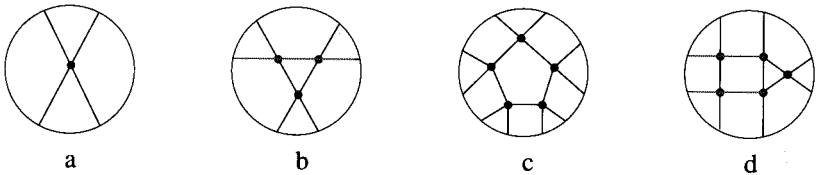


FIGURE 11

Obviously, there are no base nets with two vertices. It follows from Lemma 1 that if $v = 3$, then $d_3 = 4$. The corresponding base graph is shown in Figure 11b. The base net with three vertices is unique by Lemma 2.

When $v = 4$ system (*) has only one solution $d_3 = 4$, $d_4 = 1$, but, by Lemma 2, there are no base nets with such parameters.

BASE NETS WITH FIVE VERTICES. *There are only two base nets with five vertices; the corresponding base graphs are shown in Figures 11c and 11d.*

PROOF. When $v = 5$, system (*) has two solutions: $d_3 = 5$, $d_5 = 1$ and $d_3 = 4$, $d_4 = 2$. The base net corresponding to the first solution is a pentagon with five adjacent triangles. By Lemma 2, this net is unique (see Figure 11c). Let us construct the base net corresponding to the second solution. By the connectedness of $\mathbb{R}P^2$, one of the edges of this net is adjacent to a quadrangle and a triangle. This edge determines the net in a unique way (see Figure 11d).

BASE NETS WITH SIX VERTICES. *There exist only two base nets with six vertices; the corresponding base graphs are shown in Figures 18 and 20.*

PROOF. When $v = 6$, system (*) has three solutions: $d_3 = 6$, $d_6 = 1$; $d_3 = 5$, $d_4 = 1$, $d_5 = 1$; and $d_3 = 4$, $d_4 = 3$. By Lemma 2, there is no base net corresponding to the first solution.

Assume that there is a base net Γ corresponding to the solution $d_3 = 5$, $d_4 = 1$, $d_5 = 1$. Let us show first that its pentagon P and quadrangle Q have no common edges. Suppose P and Q have two common edges. These edges, obviously, have no common vertices. The union $P \cup Q$ is a Möbius strip. Indeed, if this is not the case, then $P \cup Q$ is an annulus. Its boundary circle bounds a disk in $\mathbb{R}P^2$ and intersects Γ in two or three points (see Figure 12). Thus this disk is divided by Γ into regions among which, despite the position of the sixth vertex of Γ , there are regions adjacent to one or two vertices. But this contradicts the assumption that Γ is a base net. Denote by D the circle $\text{Cl}(\mathbb{R}P^2 \setminus (P \cup Q))$ (see Figure 13a). Let $\Gamma' = \Gamma \cap D$ (see Figure 13b). The graph Γ' has six vertices, five of which lie in ∂D , and ten edges. Since five of these ten edges lie in ∂D and four edges are adjacent to the single inner vertex, there is an edge of which two boundary vertices lie in ∂D . Therefore, this edge divides D into two regions, one of which contains the inner vertex, and the other is a lune. But this contradicts the assumption that Γ is a base net.

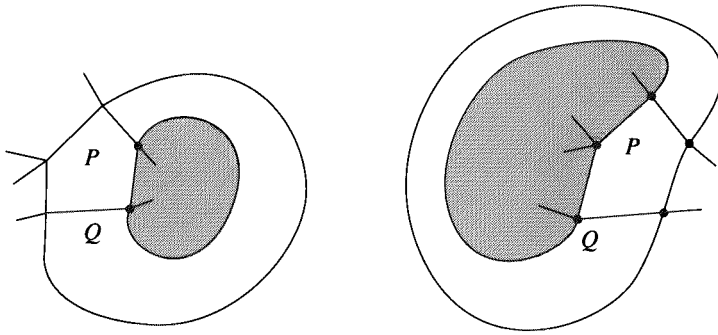


FIGURE 12

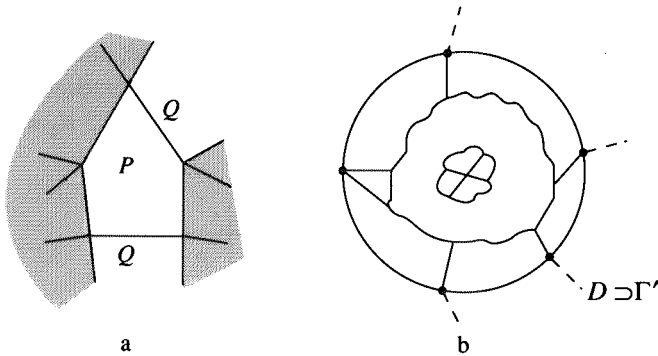


FIGURE 13

Suppose that P and Q have only one common edge. Let v be a common vertex of P and Q which does not lie in their common edge (such a vertex exists because the number of vertices is six). Let T be a triangle adjacent to v all of whose edges belong to P . Denote by D the disk $Cl(\mathbb{R}P^2 \setminus (P \cup Q \cup T))$ (see Figure 14a). Let $\Gamma' = \Gamma \cap D$ (see Figure 14b). The graph Γ' has six vertices, five of which lie in ∂D , and nine edges. Two of five boundary vertices of Γ' have three adjacent edges each, the other two vertices have two adjacent edges, and the fifth one has four adjacent edges (see Figure 14b). It is clear that in the decomposition of D by Γ there are only lunes or regions adjacent to one vertex. This contradicts the assumption that Γ is a base net. Thus, P and Q have no common edges.

Further, P and Q cannot have four common vertices. Indeed, each of the four edges adjacent to a vertex $w \notin P$ is adjacent to P at its other end point. If the intersection $P \cap Q$ consists of these four points, then at least two of these four edges are connected by w with one of the vertices of $P \cap Q$ (see Figure 15). Therefore, $w \in Q$, which is impossible. Thus, P and Q have three common vertices. Then Q and three different triangles are adjacent to $w \notin P$. Let T be the triangle among these three that is not adjacent to Q (see Figure 16). It is clear that T and P have no common edge. Since

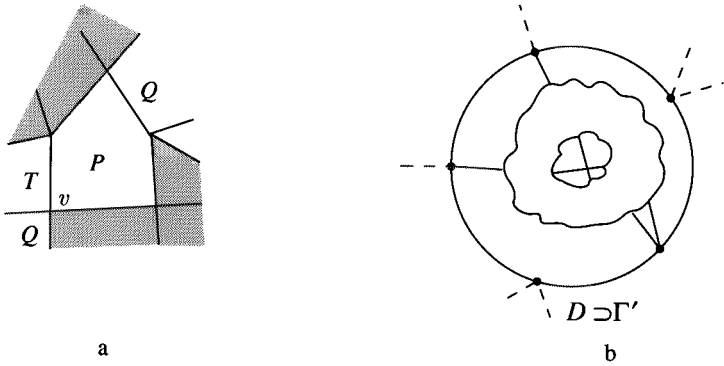


FIGURE 14

the pentagon and the quadrangle have no common edge, each of the triangles must have a common edge with the pentagon. This contradiction shows that there is no base net corresponding to the solution $d_3 = 5$, $d_4 = 1$, $d_5 = 1$.



FIGURE 15

Now consider the solution $d_3 = 4$, $d_4 = 3$. Let Γ be a base net corresponding to that solution. Denote by Q one of the quadrangles, and denote by v , w the vertices of Γ not belonging to Q . As it was noted, four different regions are adjacent to each vertex of Γ . Since the number of regions is equal to seven, for any two vertices there is a common region adjacent to them. If v and w are connected by an edge of the net, then the common region N adjacent to them is a triangle, otherwise N is a quadrangle. It is clear that N and Q are not adjacent regions. Thus the fragment of the net containing all vertices looks like Figure 17a or Figure 17b. It is not difficult to see that there are only two 6-vertex base nets having the fragment shown in Figure 17a; their base graphs are shown in Figures 18a and 18b. The graphs of Figure 18a and 18b are transformed one to the other by the moves $\tilde{\Omega}_4$, $\tilde{\Omega}_5$, see Figure 19; thus they define the same net. There is only one 6-vertex base net containing the fragment shown in Figure 17b, see Figure 20. Thus, there are only two base nets corresponding to the solution $d_3 = 4$, $d_4 = 3$. \square

All base graphs with six vertices or less are shown in Figures 21 (the graphs of Figures 11c and 11d are represented in a more convenient form). Denote these graphs by g^1 , g^3 , g_1^5 , g_2^5 , g_1^6 , g_2^6 .

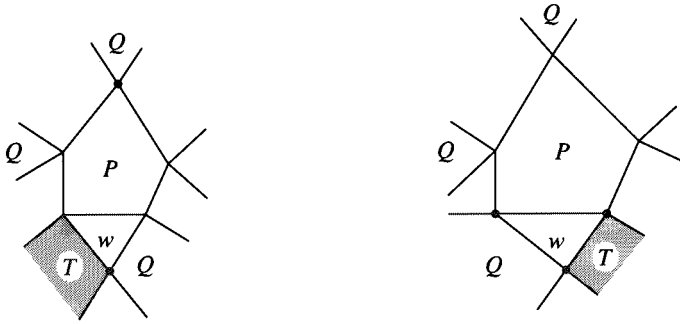


FIGURE 16

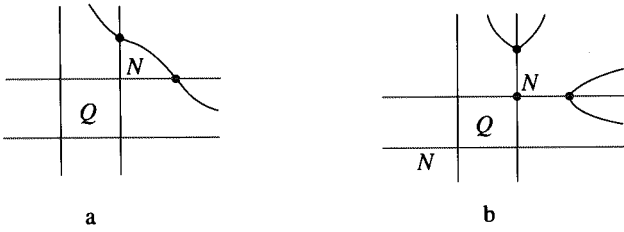


FIGURE 17

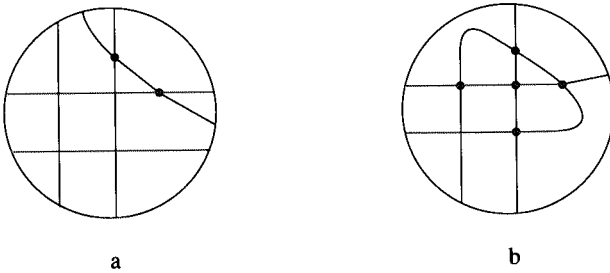


FIGURE 18

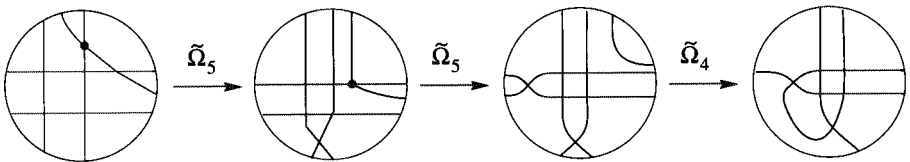


FIGURE 19

2.5. Enumeration of diagrams. The enumeration of diagrams is carried out according to the outline described in subsection 2.3. It is too cumbersome to reproduce the details here. Note that there are 126 rationally nonequivalent tangles with at most six double points.

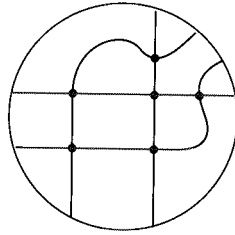


FIGURE 20

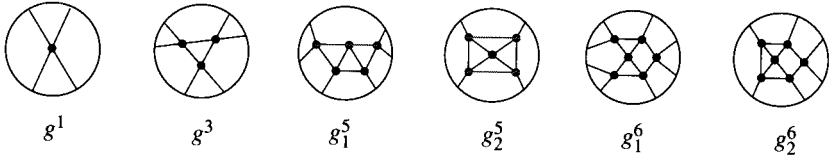


FIGURE 21

§3. The table

THEOREM. *Any nonaffine irreducible link in $\mathbb{R}P^3$ with at most six double points is isotopic to one of the links of the table or to its mirror image; the amphicheiral links (i.e., links isotopic to their mirror images) are listed at the end of the table.*

3.1. Codes of links. Denote by $\overline{p/q}$ the rational tangle $-p/q$ with $p/q > 0$. In the notation $(t_1 t_2)$ for the product of two tangles, we shall omit the brackets. Denote by (t_1, t_2, \dots, t_n) the algebraic tangle $t_1 0 + t_2 0 + \dots + t_n 0$. Denote by $\Gamma t_1 . t_2 . \dots . t_n$ the link whose diagram is obtained from the base graph Γ ($= g^1, g^3, g_1^5, g_2^5, g_1^6, g_2^6$) by inserting the tangles t_1, \dots, t_n (Figure 22 shows how they are inserted). We shall omit the symbol Γ in the cases $\Gamma = g_1$ or g_3 . For example, the link shown in Figure 9 is denoted by $\frac{3}{2} . 1 . \bar{2}$.

We also use another way of coding, similar to the one applied by Alexander and Briggs in their table [AB] of links in \mathbb{R}^3 . Denote by c'_N the link with r components having c double points which is the N th link in our table of links with given number of double points and given number of components. The superscript $r = 1$ will be omitted.

3.2. A polynomial for nonoriented links in $\mathbb{R}P^3$. Polynomials v_L for framed links $L \subset \mathbb{R}P^3$ and V_L for oriented links $L \subset \mathbb{R}P^3$ generalizing respectively the Kauffman bracket for framed links in $\mathbb{R}P^3$ and the Jones polynomial (in Kauffman's version) for oriented links in \mathbb{R}^3 are defined in [D1]. Here we define a related polynomial invariant for nonoriented links in $\mathbb{R}P^3$, which is a Laurent polynomial on one variable.

This polynomial is calculated from any link diagram. By a *state* of a

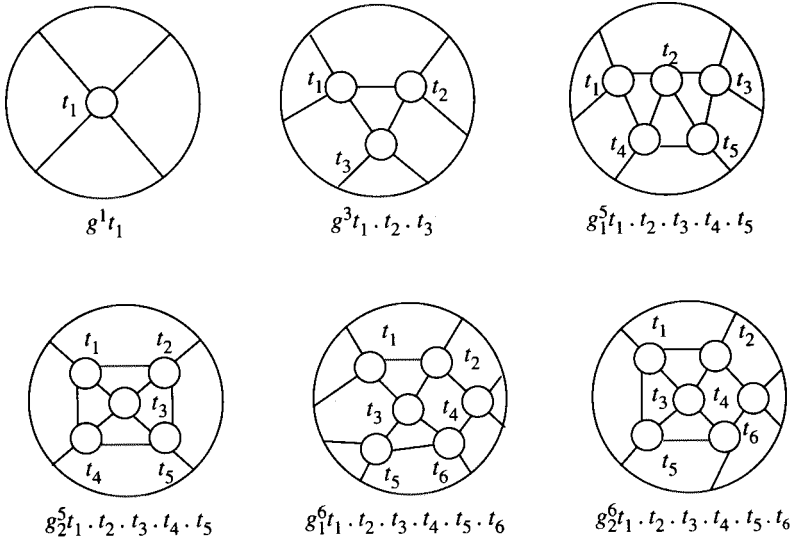


FIGURE 22

diagram we mean a choice of a pair of vertical angles at each double point. At each double point this choice can be made in two ways (see Figure 23). The chosen regions are shown by a marker (a segment connecting them). There are two types of markers: *A*-markers and *B*-markers (see Figure 23).



FIGURE 23

Let D be a diagram of a link L and s be a state of D . Denote by $a(s)$ and $b(s)$ the number of *A*-markers and *B*-markers respectively for the state s . Smooth each double point according to its marker (see Figure 24). The diagram turns into several disjoint arcs and circles and its image in the projective plane obtained from the disk of the diagram by identification of antipodal points of the boundary circle turns into several disjoint circles. Denote the number of these circles by $|s|$. Define the polynomial

$$v_L(A) = \sum_s A^{a(s)-b(s)} (-A^{-2} - A^2)^{|s|-1},$$

where the sum is taken over all states s of D . As shown in [D1], $v_L(A)$ is invariant under $\Omega_2 - \Omega_5$ and generalizes the Kauffman bracket for framed links in S^3 .

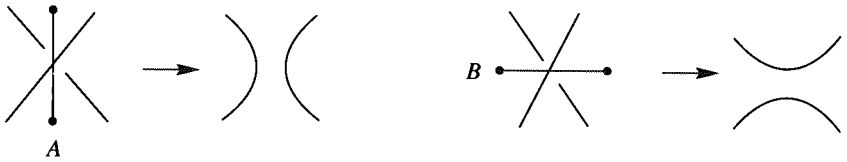


FIGURE 24

Orient L . Assign to each double point of the oriented diagram D a number ε equal to 1 or -1 depending on the type of the double point (see Figure 25). Define the *writhe* $w(D) = \sum_i \varepsilon_i$, where the sum is taken over all double points of D which are self-intersection points of the projection of the same component of L . It is clear that the writhe does not depend on the choice of orientation. Define the polynomial

$$f_L(A) = (-A)^{-3w(D)} v_L(A).$$

It is clear that $f_L(A)$ is an (ambient isotopy) invariant under $\Omega_2 - \Omega_5$. It follows easily from properties of $v_L(A)$ (see [D1]) that $f_L(A)$ is invariant under Ω_1 . Thus $f_L(A)$ is an invariant of nonoriented links $L \subset \mathbb{R}P^3$.

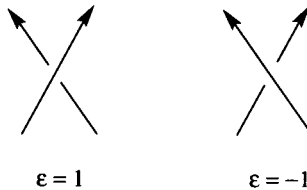


FIGURE 25

It is not difficult to define the corresponding polynomial invariant for nonoriented links $L \subset \mathbb{R}^3$. For a link contained in $\mathbb{R}^3 \subset \mathbb{R}P^3$, it coincides with f_L .

There is an obvious relationship between V_L and f_L :

$$f_L(A) = (-A)^{3w'(D)} V_L(A);$$

here $w'(D) = \sum_i \varepsilon_i$ and the sum is taken over all double points of the diagram where the projections of distinct components intersect each other.

3.3. Irreducibility and nonaffinity of table links. Let f_L and f_K be the polynomials of $L \subset \mathbb{R}P^3$ and $K \subset S^3$ respectively. Let $L \amalg K$ and $L \# K$ be the disjoint and the connected sum of L and K respectively. Then

$$f_{L \amalg K} = (-A^{-2} - A^2) f_L f_K, \quad f_{L \# K} = f_L f_K. \quad (*)$$

It is not difficult to check that all but one of the links in the table have polynomials not representable in the form (*). The only exception is the link 6_{27}^2 (see Figure 26) with polynomial $-A^{-2} - A^2$. This two-component link is irreducible because the linking number for the orientation shown is two. Therefore all links of the table are irreducible.

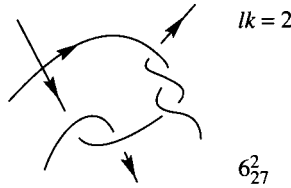


FIGURE 26

In the table there are two pairs of links with the same polynomials: the link 5_6^2 and the affine link 4_1^2 , the link 6_{24}^2 and the mirror image of the affine link 5_1^2 . The two-component links 5_6^2 , 4_1^2 , 6_{24}^2 , 5_1^2 oriented as shown in Figure 27 have linking numbers 0, 2, 2, 0 respectively. Therefore 5_6^2 is not isotopic to 4_1^2 and 6_{24}^2 is not isotopic to the mirror image of 5_1^2 . Thus all the table links are nonaffine.

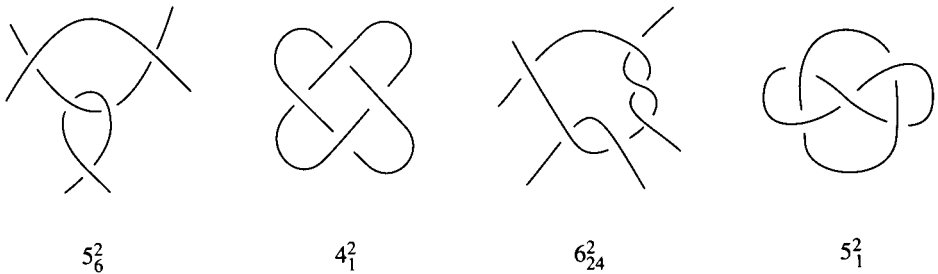


FIGURE 27

It is easy to see that each table link L with $f_L(A) = f_L(A^{-1})$ (except 6_{27}^2) is amphicheiral. The link 6_{27}^2 is not amphicheiral: removing a noncontractible component from it, we obtain the link 2 , which is not amphicheiral because its polynomial is not symmetric.

Table of links in $\mathbb{R}P^3$

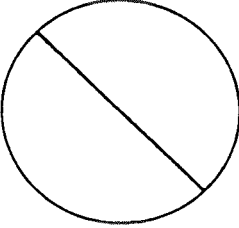
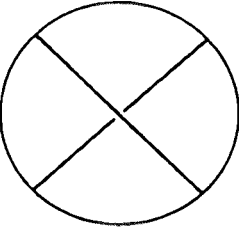
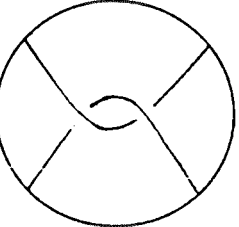
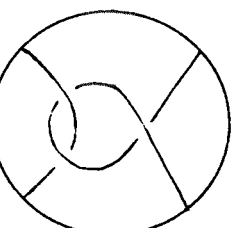
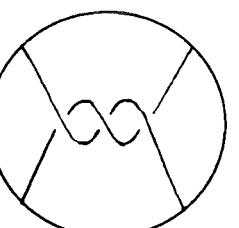
Diagram of the link	Its notation	The polynomial f_L
	0_1 (amphicheiral knot)	1
	1_1^2 1 (amphicheiral link)	$A + A^{-1}$
	2_1^2 2	$A^{-4} + A^{-6} - A^{-10}$
	3_1 $3/2$	$A^2 + 1 - A^{-2} - A^{-4} + A^{-8}$
	3_1^2 3	$A^3 + A - A^{-3} + A^{-7}$

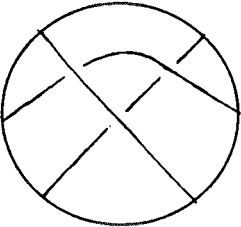
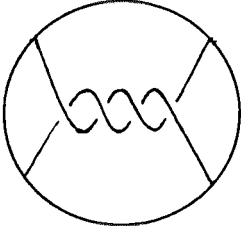
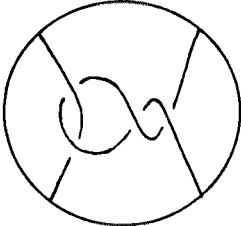
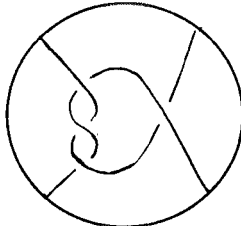
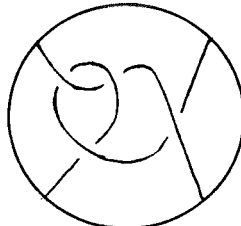
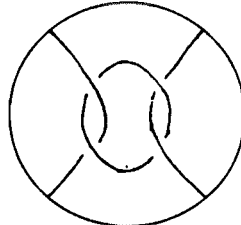
Diagram of the link	Its notation	The polynomial f_L
	3_1^3 1.1.1	$-A^5 - A - 2A^{-3}$
	4_1 4	$A^{-8} + A^{-10} - A^{-14} + A^{-18} - A^{-22}$
	4_2 5/2	$-A^{18} - A^{16} + A^{14}$ $+2A^{12} - A^8 + A^4$
	4_3 4/3	$A^{-4} + A^{-6} - A^{-8} - A^{-10}$ $+A^{-12} + A^{-14} - A^{-18}$
	4_1^2 5/3	$A^3 + A - A^{-1} - A^{-3}$ $+A^{-5} + 2A^{-7} - A^{-11}$
	4_2^2 (2, 2)	$A^8 - 2A^4 - 2A^2$ $+1 + A^{-2} - A^{-6}$

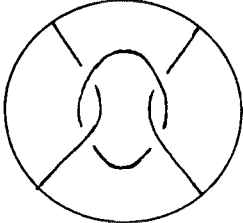
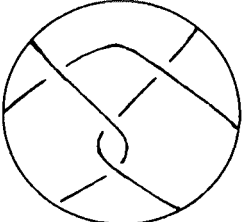
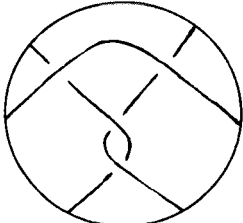
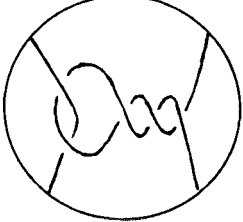
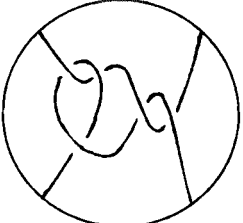
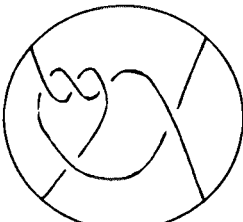
Diagram of the link	Its notation	The polynomial f_L
	$\begin{array}{c} 4_3^2 \\ (\bar{2}, 2) \\ \text{(amphicheiral link)} \end{array}$	$-A^6 - A^4 + 2 - A^{-4} - A^{-6}$
	$\begin{array}{c} 4_4^2 \\ 1.1.1/2 \end{array}$	$A^{14} - A^{10} - 2A^2$
	$\begin{array}{c} 4_5^2 \\ \bar{1}.1.1/2 \end{array}$	$A^{12} - A^8 - A^4 - 1$
	$\begin{array}{c} 5_1 \\ 7/2 \end{array}$	$\begin{array}{c} A^{10} + A^8 - A^6 \\ -2A^4 + 2 - A^{-4} + A^{-8} \end{array}$
	$\begin{array}{c} 5_2 \\ 8/3 \end{array}$	$\begin{array}{c} A^4 + A^2 - 1 - 2A^{-2} \\ + A^{-4} + 2A^{-6} \\ - 2A^{-10} + A^{-14} \end{array}$
	$\begin{array}{c} 5_3 \\ 7/4 \end{array}$	$\begin{array}{c} A^{-2} + A^{-4} - A^{-6} - A^{-8} \\ + A^{-10} + 2A^{-12} - A^{-14} \\ - 2A^{-16} + A^{-20} \end{array}$

Diagram of the link	Its notation	The polynomial f_L
	5_4 $8/5$	$-A^{12} - A^{10} + 2A^8 + 2A^6$ $-A^4 - 2A^2 + 1 + 2A^{-2} - A^{-6}$
	5_5 $5/4$	$A^2 + 1 - A^{-2} - A^{-4} + A^{-6}$ $+A^{-8} - A^{-10} - A^{-12} + A^{-16}$
	5_6 $(2, 3)$	$A^{14} - 2A^{10} - A^8 + 2A^6$ $+2A^4 - A^2 - 1 + A^{-4}$
	5_7 $(\bar{2}, 3)$	$-A^{24} - A^{22} + A^{20} + 2A^{18}$ $-2A^{14} + A^{10} + A^8$
	5_8 $(2, 3/2)$	$-A^6 + 2A^2 + 2 - 2A^{-2}$ $-2A^{-4} + A^{-6}$ $+2A^{-8} - A^{-12}$
	5_9 $2.2.1$	$A^{-8} + A^{-12} - A^{-20}$

Diagram of the link	Its notation	The polynomial f_L
	$\frac{5_{10}}{2.2.1}$	$2A^{-4} - A^{-8} + A^{-12} - 2A^{-16} + A^{-20}$
	$\frac{5_{11}}{1.2.2}$	$-A^4 + 2 + A^{-8} - A^{-12}$
	$\frac{5_2^2}{5}$	$A^5 + A^3 - A^{-1} + A^{-5} - A^{-9} + A^{-13}$
	$\frac{5_2^2}{7/3}$	$A^9 + A^7 - A^5 - 2A^3 + A + 2A^{-1} - A^{-5} + A^{-9}$
	$\frac{5_3^2}{7/5}$	$A^3 + A - A^{-1} - A^{-3} + 2A^{-5} + 2A^{-7} - A^{-9} - 2A^{-11} + A^{-15}$
	$\frac{5_4^2}{(2, 2/3)}$	$-A^{12} - A^{10} + 2A^8 + 2A^6 - A^4 - 3A^2 + A^{-2} - A^{-6}$

Diagram of the link	Its notation	The polynomial f_L
	5_5^2 1.1.2/3	$-A^{12} + A^8 - A^4 + 1 - 2A^{-4}$
	5_6^2 $\bar{1}.1.2/3$	$-A^{10} + A^6 - A^2 - A^{-6}$
	5_1^3 (2, 2)1	$-A^7 - A^5 + A^3 +$ $A - 2A^{-1} - 3A^{-3}$ $+ 2A^{-7} - A^{-11}$
	5_2^3 (2, 2) $\bar{1}$	$-A^7 - A^5 + A - 2A^{-3} - A^{-5}$
	5_3^3 1.3.1	$-A^7 - A^3 - A^{-1} - A^{-9}$
	5_4^3 $\bar{1}.3.1$	$-2A^5 - 2A^{-3} + A^{-7} - A^{-11}$

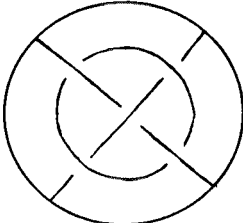
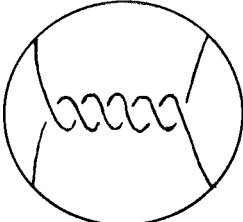
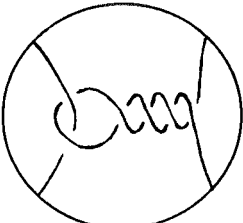
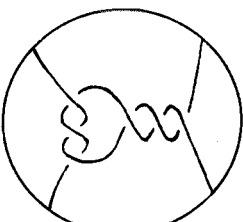
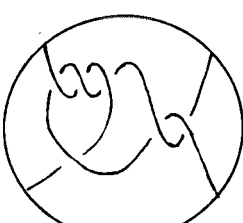

Diagram of the link	Its notation	The polynomial f_L
	$8_2^5 1.1.1.1.1$ 5_5^3 (amphicheiral link)	$A^9 - 3A^5 - 2A^3 + 2A + 2A^{-1} - 2A^{-3} - 3A^{-5} + A^{-9}$
	6_1	$A^{-12} + A^{-14} + A^{-22} - A^{-26} + A^{-30} - A^{-34}$
	6_2 $9/2$	$-A^{-26} - A^{-24} + A^{-22} + 2A^{20} - 2A^{16} + 2A^{12} - A^8 + A^4$
	6_3 $10/3$	$A^{-8} + A^{-10} - A^{-12} - 2A^{-14} + A^{-16} + 3A^{-18} - 2A^{-22} + A^{-26} - A^{-30}$
	6_4 $11/4$	$-A^{-26} - A^{-24} + A^{-22} + 2A^{20} - A^{18} - 2A^{16} + A^{14} + 3A^{12} - 2A^8 + A^4$
	6_5 $12/5$	$A^{-8} + A^{-10} - A^{-12} - A^{-14} + 2A^{-16} + 3A^{-18} - A^{-20} - 3A^{-22} + 2A^{-26} - A^{-30}$

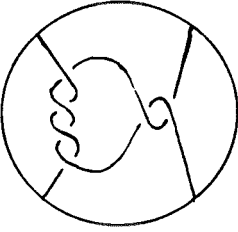
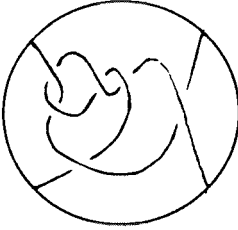
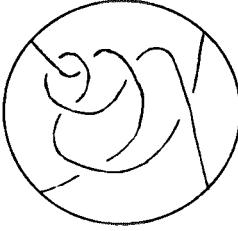
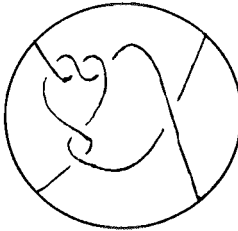
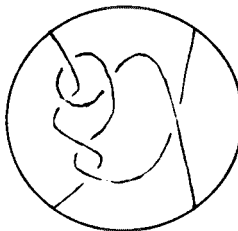
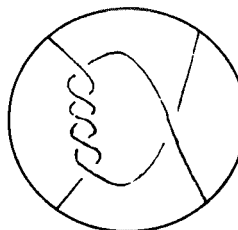
Diagram of the link	Its notation	The polynomial f_L
	6_6 $9/4$	$A^{24} - A^{22} - 2A^{20} + A^{18} + 2A^{16} - A^{12} + A^8$
	6_7 $12/7$	$A^4 + A^2 - 2 - 2A^{-2} + 2A^{-4} - 3A^{-6} - A^{-8} - 3A^{-10} + A^{-12} + 2A^{-14} - A^{-18}$
	6_8 $13/8$	$A^8 - 2A^6 - 2A^4 + 2A^2 + 3 - 2A^{-2} - 3A^{-4} + A^{-6} + 3A^{-8} - A^{-12}$
	6_9 $10/7$	$A^{-8} + A^{-10} - A^{-12} - A^{-14} + 2A^{-16} + 2A^{-18} - 2A^{-20} - 3A^{-22} + A^{-24} + 2A^{-26} - A^{-30}$
	6_{10} $11/8$	$-A^{18} - A^{16} + 2A^{14} + 2A^{12} - 2A^{10} - 2A^8 + 2A^6 + 3A^4 - A^2 - 2 + A^{-4}$
	6_{11} $6/5$	$A^{-4} + A^{-6} - A^{-8} - A^{-10} + A^{-12} + A^{-14} - A^{-16} - A^{-18} + A^{-20} + A^{-22} - A^{-26}$

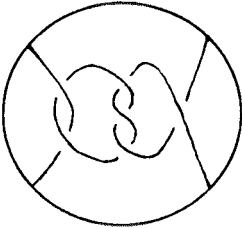
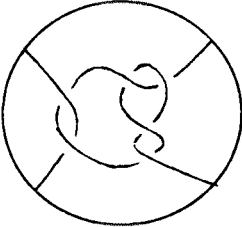
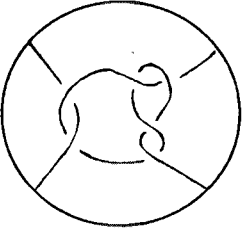
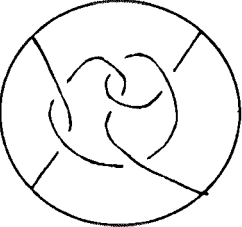
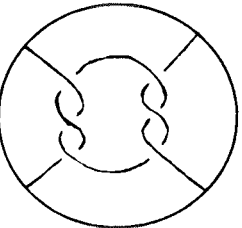
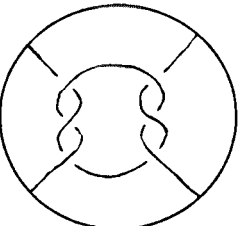
Diagram of the link	Its notation	The polynomial f_L
	6_{12} (2, 3/4)	$-A^{30} - A^{28} + 2A^{26}$ $+2A^{24} - 2A^{22} - 3A^{20}$ $+A^{18} + 3A^{16} - A^{12} + A^8$
	6_{13} (2, 5/2)	$-A^{18} + 2A^{14} + A^{12}$ $-3A^{10} - 2A^8 + 3A^6$ $+3A^4 - A^2 - 2 + A^{-4}$
	6_{14} (2, 5/2)	$A^4 + A^2 - 1 - 2A^{-2}$ $+A^{-4} + 3A^{-6} - 3A^{-10}$ $-A^{-12} + A^{-14} + A^{-16}$
	6_{15} (2, 5/3)	$-A^6 + 3A^2 + 2 - 3A^{-2}$ $-3A^{-4} + 2A^{-6} + 3A^{-8}$ $-A^{-10} - 2A^{-12} + A^{-16}$
	6_{16} (3, 3)	$A^{-4} - 2A^{-8} + 3A^{-12}$ $+2A^{-14} - 2A^{-16} - 2A^{-18}$ $+A^{-20} + A^{-22} - A^{-26}$
	6_{17} (3, 3) (amphicheiral knot)	$A^{10} + A^8 - A^6 - 2A^4$ $+3 - 2A^{-4} - A^{-6}$ $+A^{-8} + A^{-10}$

Diagram of the link	Its notation	The polynomial f_L
	$\frac{6_{18}}{(3/2, 3/2)}$	$A^{16} - 2A^{12} - 2A^{10} + 3A^8 + 3A^6 - 2A^4 - 3A^2 + 1 + 3A^{-2} - A^{-6}$
	$\frac{6_{19}}{1/2.2.2}$	$A^{16} - A^{12} - A^4 + 2$
	$\frac{6_{20}}{1/2.2.2}$	$-2A^{24} + 2A^{20} - A^{16} + 3A^{12} - 2A^8 + A^4$
	$\frac{6_{21}}{2/3.1/2.1}$	$-A^{24} + 2A^{20} - 2A^{16} + 2A^{12} - 2A^8 + 2A^4$
	$\frac{6_{22}}{2/3.1/2.1}$	$-A^{16} + 2A^{12} - A^8 + A^4 - 1 + A^{-4}$
	$\frac{6_{23}}{2/3.1/2.1}$	$A^8 - 2A^4 + 2 - A^{-4} + 2A^{-8} - A^{-12}$

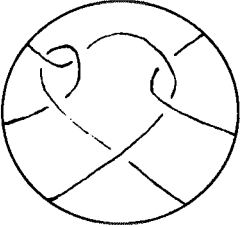
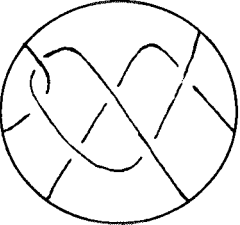
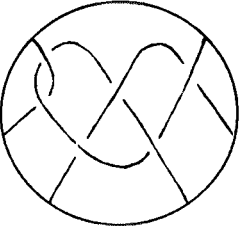
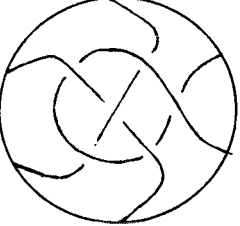
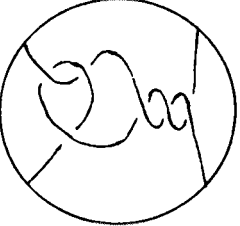
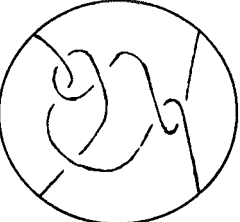
Diagram of the link	Its notation	The polynomial f_L
	${}^6_{2/3.1/2.\bar{1}}$	$A^{12} - A^8 + A^{-4}$
	$g_1^5 {}^6_{1/2.\bar{1}.1.1.1}$	$2A^8 - A^4 + 1 - 2A^{-4} + A^{-8}$
	$g_1^5 {}^6_{1/2.\bar{1}.\bar{1}.1.1}$	$2A^{12} - A^8 - 1 + A^{-4}$
	$g_2^6 {}^6_{1.1.\bar{1}.1.1.1}$	$2A^8 - 3A^4 + 2 - 2A^{-4} - 3A^{-8} - A^{-12}$
	${}^6_1/3$	$A^5 + A^3 - A - 2A^{-1} + A^{-3} + 3A^{-5} - 2A^{-9} + 2A^{-13} - A^{-17}$
	${}^6_2/5$	$-A^{13} - A^{11} + 2A^9 + 3A^7 - A^5 - 3A^3 + A + 3A^{-1} - 2A^{-5} + A^{-9}$

Diagram of the link	Its notation	The polynomial f_L
	$\frac{6^2}{9/5}$	$A^5 + A^3 - A - A^{-1} + A^{-3} + 2A^{-5} - A^{-7} - 2A^{-9} + A^{-11} + 2A^{-13} - A^{-17}$
	$\frac{6^2}{11/7}$	$A^9 + A^7 - 2A^5 - 2A^3 + 2A + 3A^{-1} - A^{-3} - 2A^{-5} + A^{-7} + 2A^{-9} - A^{-13}$
	$\frac{6^2}{9/7}$	$A^3 + A - A^{-1} - A^{-3} + 2A^{-5} + 2A^{-7} - 2A^{-9} - 2A^{-11} + A^{-13} + 2A^{-15} - A^{-19}$
	$\frac{6^2}{(2, 4)}$	$A^{14} - 2A^{10} - A^8 + 2A^6 + A^4 - 2A^2 - 2 + A^{-2} + A^{-4} - A^{-8}$
	$\frac{6^2}{(\bar{2}, 4)}$	$-A^{12} - A^{10} + A^8 + 2A^6 - A^4 - 2A^2 + 2A^{-2} - A^{-6} - A^{-8}$
	$\frac{6^2}{(2, 4/3)}$	$A^{10} - 2A^6 - 2A^4 + 2A^2 + 2 - 2A^{-2} - 3A^{-4} + A^{-6} + 2A^{-8} - A^{-12}$

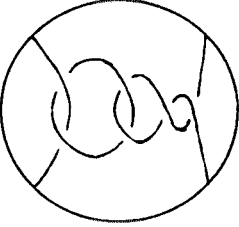
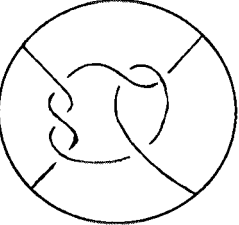
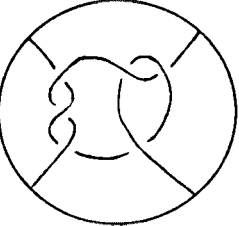
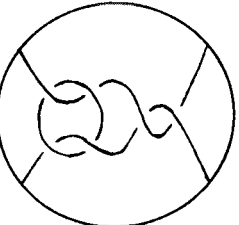
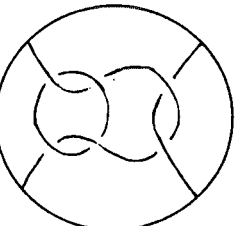
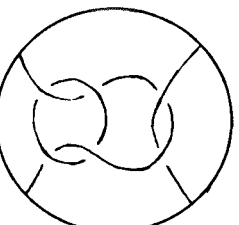
Diagram of the link	Its notation	The polynomial f_L
	6_9^2 (2, 2/5)	$A^{16} + A^{14} - 2A^{12}$ $-3A^{10} + A^8 + 3A^6$ $-3A^2 + A^{-2} - A^{-6}$
	6_{10}^2 (3, 3/2)	$A^9 - 2A^5 - A^3 + 3A$ $+3A^{-1} - 2A^{-3} - 2A^{-5}$ $+A^{-7} + 2A^{-9} + A^{-13}$
	6_{11}^2 (3, 3/2)	$A^5 + A^3 - 2A^{-1}$ $+3A^{-5} + A^{-7} - 2A^{-9}$ $-2A^{-11} + A^{-13} + A^{-15}$
	6_{12}^2 (2, 2)2	$-A^2 - 1 + A^{-2} + 2A^{-4}$ $-2A^{-6} - 3A^{-8} + 3A^{-12}$ $-2A^{-16} + A^{-20}$
	6_{13}^2 (2, 2)1/2	$A^{16} - 2A^{12} - 2A^{10}$ $+3A^8 + 3A^6 - 2A^4$ $-4A^2 + 2A^{-2} - A^{-6}$
	6_{14}^2 (2, 2)1/2	$-A^2 - 1 + 2A^{-4}$ $-3A^{-8} - 2A^{-10} + 2A^{-12}$ $+2A^{-14} - A^{-18}$

Diagram of the link	Its notation	The polynomial f_L
	6_{15}^2 $(2, 3)1$	$A^{-1} + A^{-3} - A^{-5} - A^{-7}$ $+ 2A^{-9} + 3A^{-11} - A^{-13}$ $- 3A^{-15} + 2A^{-19} - A^{-23}$
	6_{16}^2 $(2, 3/2)1$	$-A^{19} - A^{17} + 2A^{15}$ $+ 2A^{13} - 2A^{11} - 3A^9$ $+ 2A^7 + 4A^5 - 2A + A^{-3}$
	6_{17}^2 $(2, 2)11$	$-A^6 - A^4 + 2A^2 + 2$ $- 3A^{-2} - 3A^{-4} + A^{-6}$ $+ 3A^{-8} - A^{-10}$ $- 2A^{-12} + A^{-16}$
	6_{18}^2 $1.1.4$	$-A^{-4} - A^{-8} - A^{-12} + A^{-24}$
	6_{19}^2 $\bar{1}.1.4$	$-2A^{-6} - 2A^{-14}$ $+ 2A^{-18} - A^{-22} + A^{-26}$
	6_{20}^2 $1.\bar{1}.4/3$	$-2A^{22} + A^{18} - 2A^{14}$ $+ A^{10} - A^6 + A^2$

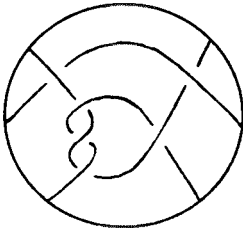
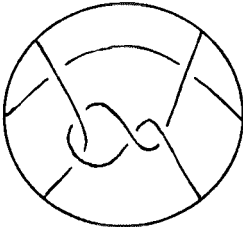
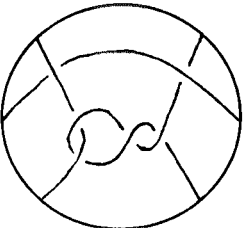
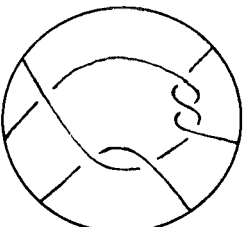
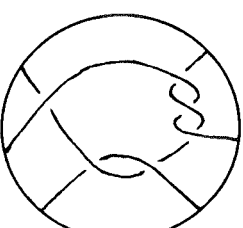
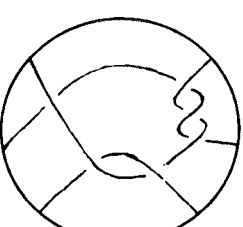
Diagram of the link	Its notation	The polynomial f_L
	$\frac{6_{21}^2}{1.1.4/3}$	$A^{-4} - A^{-8} + A^{-12} - 2A^{-16} - A^{-24}$
	$\frac{6_{22}^2}{1.1.5/2}$	$2A^{20} - 2A^{16} + A^{12} - 3A^8 + A^4 - 1$
	$\frac{6_{23}^2}{1.1.5/2}$	$-A^{-2} - 2A^{-10} + A^{-22}$
	$\frac{6_{24}^2}{1.1/3.2}$	$-A^6 + A^2 - 2A^{-2} + A^{-6} - 2A^{-10} + A^{-14}$
	$\frac{6_{25}^2}{1.1/3.2}$	$-A^4 + 1 - 2A^{-4} - A^{-12} + A^{-16}$
	$\frac{6_{26}^2}{1.1/3.2}$	$-2 + A^{-4} - 2A^{-8} + 2A^{-12} - 2A^{-16} + A^{-20}$

Diagram of the link	Its notation	The polynomial f_L
	6^2_{27} $1.1/3.\bar{2}$	$-A^2 - A^{-2}$
	6^2_{28} $2.2.2$	$-A^8 - A^4 + 1 - A^{-12}$
	6^2_{29} $2.2.\bar{2}$	$A^8 - 3A^4 + 1 - 2A^{-4}$ $+ 2A^{-8} - A^{-12}$
	6^2_{30} $g_2^5 1.1.\bar{1}.2.1$	$-A^7 + 3A^3 + 2A - 3A^{-1}$ $- 3A^{-3} + 3A^{-5} + 4A^{-7}$ $- A^{-9} - 3A^{-11} + A^{-15}$
	6^2_{31} $g_2^5 \bar{1}.1.1.2.1$	$A^{-1} + A^{-3} - A^{-7}$ $+ 2A^{-11} + A^{-13}$ $- A^{-15} - A^{-17}$
	6^2_{32} $g_2^5 1.\bar{1}.1.2.\bar{1}$	$A^{-3} + 2A^{-5} - 2A^{-9}$ $+ 2A^{-13} + A^{-15}$ $- A^{-17} - A^{-19}$

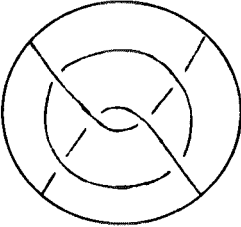
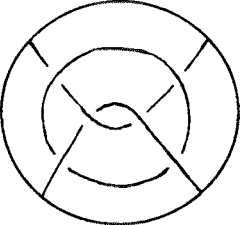
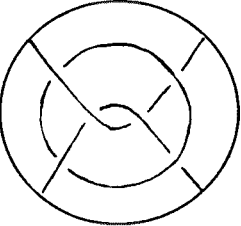
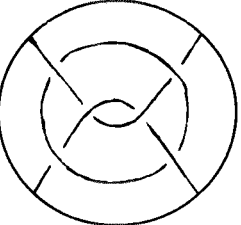
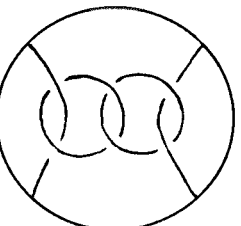
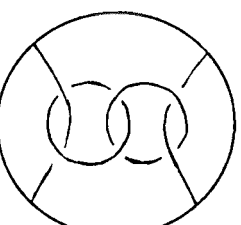
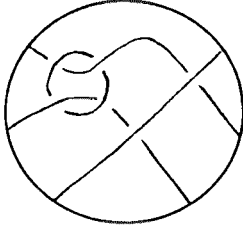
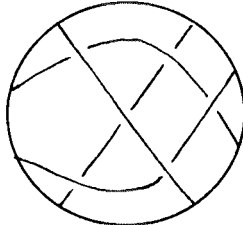
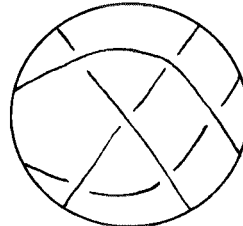
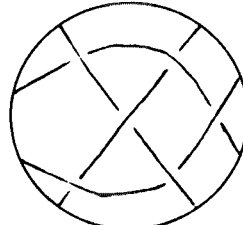
Diagram of the link	Its notation	The polynomial f_L
	6_{33}^2 $g_2^5 1.1.2.1.1$	$-2A^{-2} - A^{-4} + A^{-6}$ $+A^{-8} - A^{-10}$ $-A^{-12} + A^{-16}$
	6_{34}^2 $g_2^5 \bar{1}.1.2.\bar{1}.1$	$-1 - 2A^{-2} + A^{-4}$ $+2A^{-6} - 3A^{-10} - A^{-12}$ $+A^{-14} + A^{-16}$
	6_{35}^2 $g_2^5 1.1.2.\bar{1}.\bar{1}$	$-A^2 - 1 + A^{-4}$ $-A^{-8} - A^{-10} + A^{-12}$
	6_{36}^2 $g_2^5 1.1.\bar{2}.1.1$	$-A^{18} + 3A^{14} + 2A^{12}$ $-4A^{10} - 3A^8 + 2A^6$ $+3A^4 - 2A^2 - 3 + A^{-4}$
	6_1^3 $(2, 2, 2)$	$-A^{12} + 3A^8 + 3A^6$ $-3A^4 - 3A^2 + 1$ $+4A^{-2} - A^{-6} + A^{-10}$
	6_2^3 $(2, \bar{2}, 2)$	$A^{10} + A^8 - 3A^4$ $+3 + 3A^{-2} - A^{-4}$ $-A^{-6} + A^{-10}$

Diagram of the link	Its notation	The polynomial f_L
	6_3^3 (2, 2, 1)1	$-A^7 - A^5 + A^3$ $+ A - 3A^{-1} - 3A^{-3}$ $+ 2A^{-5} + 3A^{-7} - A^{-9}$ $- 3A^{-11} + A^{-15}$
	6_4^3 1.1.5/3	$-2A^5 + A - 3A^{-3}$ $+ A^{-7} - 2A^{-11} + A^{-15}$
	6_5^3 1.1.5/3	$A^{13} - 2A^9 - 2A - A^{-7}$
	6_6^3 (2, 2).1.1 (amphicheiral link)	$2A^8 - A^4 + 2 - A^{-4} + 2A^{-8}$
	6_7^3 (2, 2).1.1	$-A^{10} + 3A^6 + 2A^{-2}$ $- A^{-6} + A^{-10}$
	6_8^3 (2, 2).1.1 (amphicheiral link)	$A^{10} + A^6 + A^{-6} + A^{-10}$

Diagram of the link	Its notation	The polynomial f_L
	6_9^3 $(2, 2). \bar{1}. \bar{1}$	$-A^{12} + 2A^8 + 3$ $-A^{-4} + A^{-8}$
	6_1^4 $g_1^6 1.1.1. \bar{1}. \bar{1}. 1.1$ <p>(amphicheiral link)</p>	$-A^6 - 2A^4 - A^2$ $-A^{-2} - 2A^{-4} - A^{-6}$
	6_2^4 $g_1^6 \bar{1}. 1. 1. 1. \bar{1}. 1. 1$	$-2A^4 - 3A^2 - 1$ $-A^{-6} - A^{-8}$
	6_3^4 $g_1^6 1.1. \bar{1}. \bar{1}. 1. 1$	$A^{10} - 4A^6 - 3A^4$ $+ 3A^2 + 3 - 4A^{-2}$ $- 6A^{-4} + 3A^{-8} - A^{-12}$

Amphicheiral links: $0_1, 1_1^2, 4_3^2, 5_5^3, 6_{17}, 6_6^3, 6_8^3, 6_1^4$.

REFERENCES

- [AB] J. W. Alexander and G. B. Briggs, *On types of knotted curves*, Ann. of Math. (2) **28** (1927), 562–586.
- [C] J. H. Conway, *An enumeration of knots and links, and some of their algebraic properties*, Computational Problems of Abstract Algebra (Proc. Conf., Oxford, 1967), Pergamon, Oxford, 1970, pp. 329–358.
- [D1] Yu. V. Drobotukhina, *An analogue of the Jones polynomial for links in $\mathbb{R}P^3$ and a generalization of the Kauffman-Murasugi theorem*, Algebra i Analiz **2** (1990), no. 3, 171–191; English transl., Leningrad Math. J. **2** (1991), no. 3, 613–630.
- [D2] ———, *Classification of projective Montesinos links*, Algebra i Analiz **3** (1991), no. 1, 118–130; English transl., St. Petersburg Math. J. **3** (1992), no. 1, 97–107.

LOMI, ST. PETERSBURG